A&A 475, 747–754 (2007)
DOI: 10.1051/0004-6361:20077914

Astronomy & Astrophysics

Spectral properties of nine M-type asteroids

M. Birlan[1], P. Vernazza[2], and D. A. Nedelcu[1,3]

[1] Institut de Mécanique Céleste et de Calcul des Éphémérides (IMCCE), Observatoire de Paris, 77 avenue Denfert-Rochereau, 75014 Paris Cedex, France
e-mail: Mirel.Birlan@imcce.fr
[2] LESIA, Observatoire de Paris-Meudon, 5 place Jules Janssen, 92195 Meudon Cedex, France
e-mail: Pierre.Vernazza@obspm.fr
[3] Astronomical Institute of the Romanian Academy, 5 Cu titul de Argint, 75212 Bucharest, Romania
e-mail: nedelcu@imcce.fr

Received 19 May 2007 / Accepted 27 August 2007

ABSTRACT

Aims. We present spectroscopic results for nine M-type asteroids (325 Heidelberga, 497 Iva, 558 Carmen, 687 Tinette, 766 Moguntia, 860 Ursina, 909 Ulla, 1280 Baillauda, and 1564 Srbija) in the 0.8−2.5 μm spectral region. One visible spectrum is also presented for the asteroid 497 Iva. These asteroids were observed during several runs between 2003 and 2007, and the main goal was to investigate the NIR spectral region of M-type asteroids.
Methods. The data was obtained with SpeX/IRTF in Prism mode and Dolores/TNG in LR-B mode. Spectral analysis was performed by comparing the M-type spectra and the meteorite ones (χ^2 approach) and the Modified Gaussian Model.
Results. With one exception, the asteroids present positive slopes of the spectra, with no absorption features, in good agreement with the spectra of metallic meteorites. The analysis of the asteroid 766 Moguntia was done by means of χ^2, MGM techniques, and the Shkuratov scattering law. We conclude that the mineralogy is dominated by olivine. Its NIR spectrum is similar to those of CO/CV meteorites.

Key words. minor planets, asteroids

1. Introduction

The M-type asteroid class was initially defined by seven parameters directly measurable from four observational techniques, namely photometry, polarimetry, radiometry and spectrophotometry (Bowell et al. 1978). Historically, this taxonomic class brought an end to previous ideas concerning bimodality in the asteroid population, largely dominated by the C-type asteroids (associated with carbonaceous materials) and the S-type ones (associated with silicate minerals).

Several articles confirmed this taxonomic class. Between 1984 and 1994 several articles reinforced the definition of the M taxonomic class (Tholen 1984; Barucci et al. 1987; Tholen & Barucci 1989; Tholen 1989; Fulchignoni et al. 1995), with various statistical tests combined with cluster analysis techniques. The analyzed colors revealed a taxonomic class with a slightly positive spectral slope, and a moderate thermal albedo (0.151 ± 0.063 in Birlan et al. 1996). This M class has been degenerated into the so-called X-complex when the thermal albedo is not taken into account.

Several results of polarimetric surveys have been published (Belskaya et al. 1985, 1987; Lupishko & Belskaya 1989; Belskaya et al. 1991; Gil-Hutton 2007). Lupishko & Belskaya (1989) give a wide range of polarimetric measurements for M-type asteroids, inconsistent with only a metallic composition of their surface. Magri et al. (2007) also found a wide interval of radar albedos among M-asteroids, again in disagreement with metal-rich surfaces for some M-type objects. Belskaya & Lagerkvist (1996) synthesized the knowledge for all M or M-like asteroids, based on colors, spectrophotometry, polarization parameter, and radiometry. They proposed a classification for these objects (the last column in their Table 1).

Lightcurve investigations of M-type asteroids (Lagerkvist et al. 1998) revealed an excess of fast rotators among them compared to other taxonomic types. According to Harris (1979), a tendency towards more rapid rotation among asteroids must be interpreted as indicating high material strength.

Various approaches of mass determination (bulk density respectively) of M-asteroids gave contradictory results. The bulk density estimation a few of them revealed very low values (Ostro et al. 2002; Margot & Brown 2003; Birlan 2000). These results imply very high values for the bulk porosity (Britt & Consolmagno 2000), that is difficult to reconcile with high strength materials.

All these references brings forth the conclusion that M-type objects are still important in deciphering the history of formation and evolution of the main belt.

It is important to mention the limitations of taxonomical classes designation, as long as the classification could not reveal the real geologic diversity that occurs among the main-belt asteroids. It is now accepted that spectroscopy provides data which are relevant for obtaining results concerning the mineralogy and chemical interpretation of atmosphereless bodies.

Spectra of M-type asteroids are consistent with the presence of Fe-bearing minerals (or metallic surfaces) and usually they are interpreted as parent bodies of metallic meteorites (Dollfus et al. 1979; Cloutis et al. 1990a,b). This interpretation is also supported by radar observations, where the strength of the reflected radar echoes is consistent with a high concentration of metals on their surfaces (e.g. Ostro et al. 2000; Magri et al. 2007).

Table 1. Date of observations with the fraction of the day for the beginning of the observation, number and name of the asteroid, semimajor axis, eccentricity, inclination, the apparent magnitude, phase angle, as well as heliocentric and geocentric distance.

Date (UT)	Asteroid	a	e	i	V	Φ (°)	r (UA)	Δ (UA)
2003/10/29.911	497 Iva	2.85918514	0.296270	4.811626	12.05	4.2	2.03	1.04
2003/11/04.482	497 Iva	2.85918514	0.296270	4.811626	12.26	6.4	2.06	1.08
2003/11/05.612	766 Moguntia	3.02032355	0.092544	10.078727	14.78	17.6	2.74	2.07
2003/11/05.630	558 Carmen	2.90676856	0.043101	8.365791	14.29	20.8	2.78	2.54
2006/04/18.226	860 Ursina	2.79537340	0.109044	13.314103	15.81	18.6	3.10	2.75
2006/04/18.321	325 Heidelberga	3.20389760	0.167631	8.540609	14.22	19.4	2.83	2.32
2006/04/18.408	1564 Srbija	3.17462507	0.199762	11.018214	16.27	4.3	3.70	2.72
2006/04/19.353	1280 Baillauda	3.41409115	0.060099	6.457478	16.10	12.9	3.56	2.86
2006/04/19.406	687 Tinette	2.72578375	0.271155	14.853600	16.90	7.4	3.43	2.50
2007/03/13.552	909 Ulla	3.54127850	0.099305	18.747663	15.03	10.6	3.89	3.14

Meanwhile Hardersen et al. (2005) claimed weak absorption features around 0.9 μm for six M-types asteroids. They associate the presence of this band with iron-poor orthopyroxenes and proposed four possible interpretations for these asteroids.

For some M-type asteroids, spectroscopic studies in the Near-InfraRed (NIR) region revealed the presence of hydrated minerals, which is difficult to explain for an evolved (constituted by melted minerals) object. Thus, based on 3-μm observations, Rivkin et al. (2000) and Rivkin et al. (1995) proposed the split of this class into "M-class" asteroids (e.g. the absence of the 3-μm absorption band) and "W-class" asteroids (e.g. hydrated ones). However Gaffey et al. (2002) discussed the observational difficulties associated with obtaining reliable spectra for the 3-μm spectral region, and proposed alternative explanations to the aqueous alteration.

In this paper we present spectroscopic results for nine M-type targets in the 0.8−2.5 μm region. The asteroids were observed during several runs between 2003 and 2007, to study M-type members in the NIR spectral region.

2. The observing protocol

The asteroids were observed in the 0.8−2.5 μm spectral region with SpeX/IRTF instrument, located on Mauna Kea, Hawaii. These observations were performed in remote mode from Centre d'Observation à Distance en Astronomie à Meudon (CODAM) (Birlan et al. 2004, 2006) using the low resolution Prism mode ($R = 100$) of the spectrograph. We used a 0.8×15 arcsec slit oriented North-South. The spectra for the asteroid and the solar analog stars were obtained alternatively on two separated locations on the slit denoted A and B (the *nodding* procedure). The data reduction process consists of two main steps: 1) obtaining the raw spectra for the object and the solar analog and 2) computation of a normalized reflectance spectrum by dividing the asteroid spectrum by the solar analog spectrum and performing a correction for telluric lines.

For the first step, the Image Reduction and Analysis Facility (IRAF `http://iraf.noao.edu`) was used in conjunction with a script that creates the command files for a specific set of IRAF instructions. For the second step, after the wavelength calibration, specific IDL routines were also used in order to diminish the influence of telluric bands in our spectra (Rivkin et al. 2004). For publish high confidence data, the raw images were re-reduced using Spextool (Cushing et al. 2004) and specific MIDAS procedures, and the results were compared with the previous ones.

Our strategy was to observe all asteroids as close to the zenith as possible (Table 2). We managed to observe all targets with an airmass of less then 1.25. No other correction for the differential refraction was performed. Each observed asteroid was preceded by observations of solar analogs in the vicinity (airmass differences between the asteroid and the standard were less than 0.1). The seeing varied between 0.7−1.8 arcsec during the observing runs, and the humidity was in the 25%−85% range.

In order to obtain a S/N in the 80−200 range, we needed 15 to 40 min of exposure time, depending on the asteroid magnitude, and counting both the effective exposure and CCD camera readout time. Exposure times are presented in Table 2.

For 497 Iva, one visible spectrum was obtained using the Dolores/TNG facility. The Dolores spectrograph was used in the LR-B mode. MIDAS procedures for spectral reduction were used for the final spectrum.

For the asteroid spectra, the solar analogs SA 93-101, HD 76332, SA 98-1155, SA 93-1077, HD 103529, HD 95364, HD 103529, HD 257880 were observed. For the computation of the final reflectance (ratio between the asteroid spectrum and the star spectrum) we took into account the similar dynamic regimes of the detector (Vacca et al. 2004; Rayner et al. 2003).

3. Results

The M-type asteroids observed are: 325 Heidelberga, 497 Iva, 558 Carmen, 687 Tinette, 766 Moguntia, 860 Ursina, 909 Ulla, 1280 Baillauda, and 1564 Srbija. Their orbital elements the observations are presented in Table 1.

The near-IR spectra are presented in Fig. 1. All the spectra are normalized to 1.21 μm. Most asteroids have linear, featureless spectra, with positive slopes. The only exception is the spectrum of 766 Moguntia, which will be treated separately.

For all the spectra we computed the slope using a linear procedure over the entire NIR spectral region.

3.1. 325 Heidelberga

Visible spectrophotometry of this object was obtained in the *24-color Survey* (Chapman & Gaffey 1979). Its IRAS albedo (Tedesco & Veeder 1992) is estimated to be 0.1068 ± 0.005 for a diameter of 75.72 ± 1.7 km. Its NIR spectrum is linear with a positive slope estimated as 0.27 μm^{-1}.

3.2. 497 Iva

This asteroid was observed in both *ECAS* (Zellner et al. 1985) and *SCAS* (Clark et al. 1995) surveys. The results of Rivkin et al. (1995) revealed no presence of water of hydration in the 3 μm

Table 2. Exposure data for each asteroid. The columns show the mean UT value for each series, the individual time for each spectrum (Itime), the number of cycles, and the airmass at the mean UT of each series.

Object	UT (h m s)	Itime(s)	Cycles	Airmass	S/N	Telescope
325 Heidelberga	07 43 16	120	10	1. 090	200	IRTF
497 Iva	21 53 10	900	1	1.037	90	TNG
497 Iva	11 34 25	30	8	1.244	110	IRTF
558 Carmen	15 07 09	40	12	1.036	200	IRTF
687 Tinette	09 45 45	120	9	1.278	70	IRTF
766 Moguntia	14 42 27	40	9	1.050	100	IRTF
860 Ursina	05 25 22	120	9	1.007	100	IRTF
909 Ulla	13 15 40	120	4	1.034	90	IRTF
1280 Baillauda	08 28 40	120	11	1.139	90	IRTF
1564 Srbija	09 47 44	120	10	1.071	70	IRTF

region. Our spectrum in the visible region (Fig. 2) has a monotonic, featureless trend, the slope being estimated as 0.36 μm^{-1}.

Its near-IR spectrum also presents a positive slope, with a value of 0.32 μm^{-1}.

3.3. 558 Carmen

Both *ECAS* and *24-color Survey* data have been reported for this asteroid. Its IRAS albedo is estimated to 0.1161 ± 0.007 for a diameter of (59.31 ± 1.8) km. Visible spectrum was given in the *S3OS2* database (Lazzaro et al. 2004).

For our NIR reddish, featureless spectrum, a slope of 0.256 μm^{-1} was computed.

3.4. 687 Tinette

Colors for *ECAS* and visible spectroscopy from *SMASS II* (Bus & Binzel 2002) have been reported. Our NIR spectrum has a positive slope with a value of 0.25 μm^{-1} and no major features of absorption.

3.5. 766 Moguntia

Colors of this asteroid were given in the *ECAS* data. No spectral data are available in the literature. However, Hardersen et al. (2006) have reported observations of this asteroid in the NIR spectral range, with an absorption band, quite unusual for M-type asteroids. Our NIR spectrum reveals a relative neutral trend with slightly positive slope of 0.065 μm^{-1}, as well as a shallow large band around 1 μm.

3.6. 860 Ursina

ECAS colors have been reported, and its IRAS albedo is estimated to 0.1618 ± 0.020 for a diameter of (29.32 ± 1.6) km. A visible spectrum obtained by the *SMASS II* survey is also available for this asteroid. Our NIR data reveal a spectrum with no significant absorption features. The slope was estimated to be 0.21 μm^{-1}.

3.7. 909 Ulla

Colors for this asteroid were observed in both *ECAS* and the *24-color asteroid Survey*. The IRAS albedo is estimated to 0.0343 ± 0.001 for a diameter of (116.44 ± 2.4) km. The estimation obtained for the IRAS albedo is close to the C or D-type asteroids than to the average value of M-type ones. The NIR spectrum was previously published by Clark et al. (2004) and exhibits a reddish trend, having a slope of 0.16 μm^{-1}.

Our NIR spectrum confirms the reddish, neutral trend for 909 Ulla, and the slope parameter was estimated to be 0.15 μm^{-1}.

3.8. 1280 Baillauda

Its IRAS albedo is smaller than the average value of M-type asteroids 0.0505 ± 0.004 for a diameter of (50.83 ± 2.0) km. *ECAS* colors are also available. The visible spectrum was obtained in the $S3OS2$ survey.

Our NIR spectrum is redish, and featureless, with a slope of 0.27 μm^{-1}.

3.9. 1564 Srbija

Only *ECAS* colors have been published for this asteroid. Our NIR spectrum is reddish, and featureless, with a slope of 0.24 μm^{-1}.

4. Discussion

Eight of our spectra (except that of 766 Moguntia) have quite large positive slopes (Fig. 6 and Table 3). For five objects (497, 687, 909, 1280, 1564) the spectra do not show any spectral features. Nevertheless, some weak bands appear in the spectra of 325 Heidelberga, 558 Carmen and 860 Ursina. Reducing the data with Spextool v3.4 did not reveal these bands. Therfore, we attribute these bands to the procedure that corrects for the telluric bands. For a few of them, the spectra have a slight modification (decreasing trend) of the slope in the region 2.3−2.5 μm which is in the region of low sensitivity of the detector (i.e. low S/N ratio).

Five of our asteroids (325, 497, 558, 766, and 860) are present in the analysis of Belskaya & Lagerkvist (1996). They classified four of them as M-type, and 766 Moguntia was considered as "unusual M".

The 3 μm region of the spectra for our targets is not present in the literature, except for that of 497 Iva, classified as anhydrous by Rivkin et al. (1995).

Polarimetric results have been published for 558 Carmen (Gil-Hutton 2007). These results are in agreement with those previously obtained for M-type asteroids. However, we note the discrepancy between its derived polarimetric albedo (0.21 ± 0.003) and the IRAS one (0.116 ± 0.007).

Hardersen et al. (2005) suggested evidence for the presence of iron-poor orthopyroxenes on the surface of some M-type asteroids. They also observed the asteroid 325 Heidelberga, but did

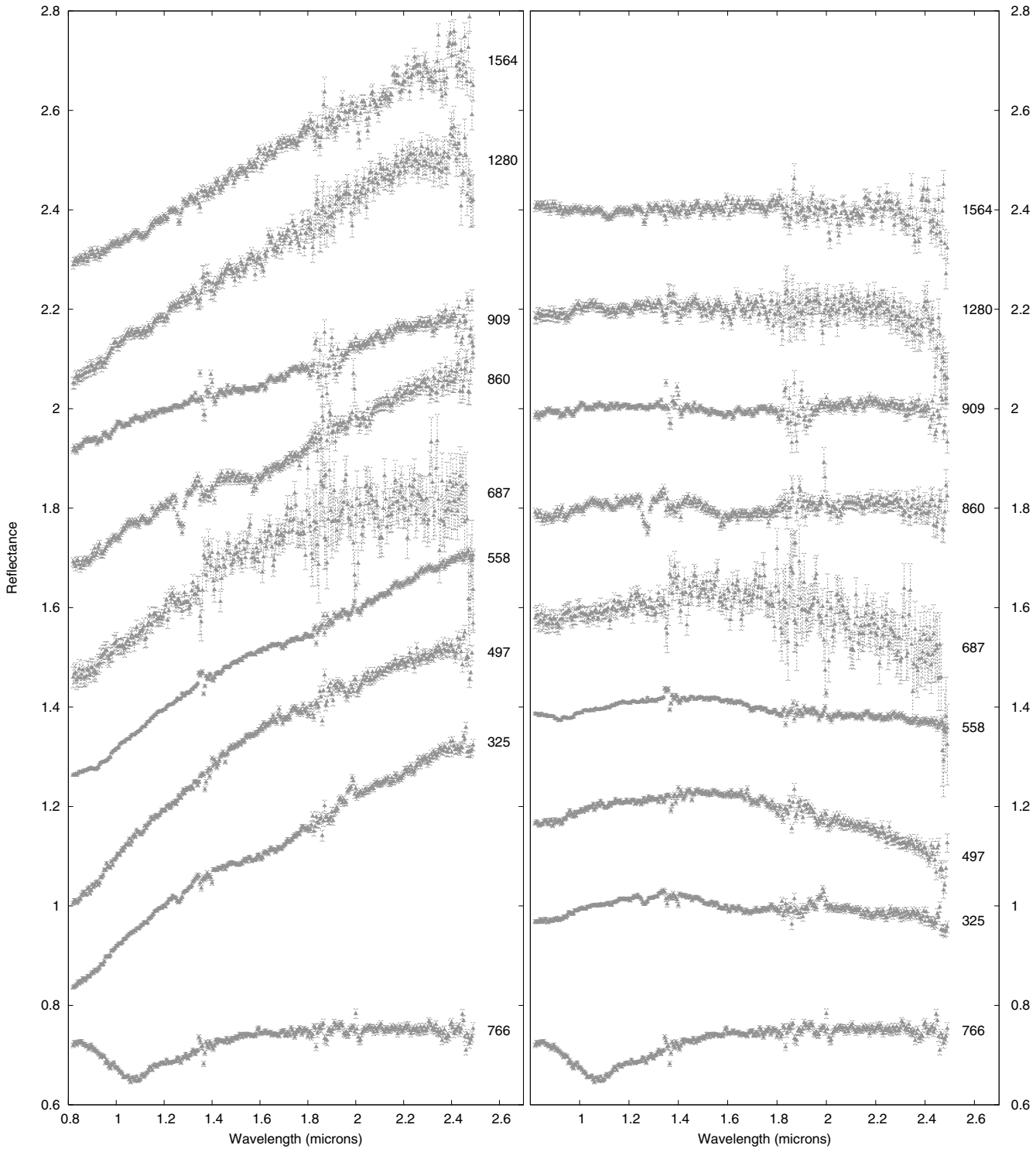

Fig. 1. NIR spectra of the nine observed asteroids, with theirs errorbars. The spectra were normalized to 1.25 μm and offset for visibility (*left panel*). Continuum subtracted spectra are presented in the *right panel*.

not find evidence for absorption bands (within the noise limit of their data). Our spectrum does not show evidence of an absorption band mainly because our observations were not conducted in this direction. This weak absorption band was also reported for the asteroids 558 Carmen (Hardersen et al. 2006) and 497 Iva (P. Hardersen, private communication).

In order to constrain the surface composition of the observed asteroids, we compared their spectra with meteorites. The RELAB database (`http://lf314-rlds.geo.brown.edu`) of meteorite spectra was used. A χ^2 analysis was performed following Nedelcu et al. (2007), identically to their work.

Several simulations were performed besides the computation of the χ^2 results presented here, we applied a χ^2 analysis to the NIR range. The NIR positive slopes of our asteroid spectra made the interpretation difficult, since several distinct and dichotomic meteorite classes (CI/CM represented by Tagish Lake, Abee, ...) have the same trend in this spectral range. Our results suggest that in this range it might be difficult to distinguish between a D,

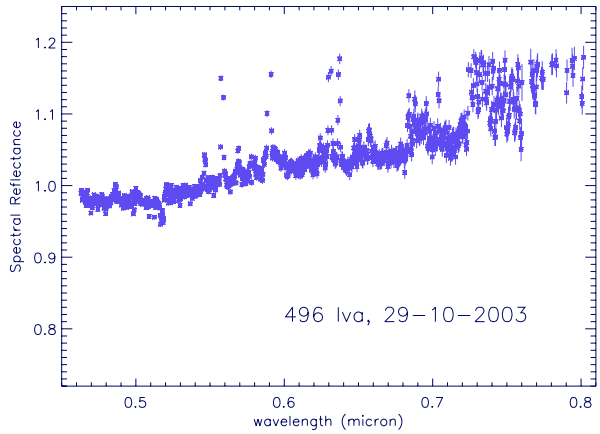

Fig. 2. The spectrum of 497 Iva in the visible region, with errorbars. This spectrum exhibits monotonic behavior with a slightly positive slope. The edge of the spectrum is less reliable because of limitations of the instrument and detector (`http://www.tng.iac.es/instruments/lrs/`).

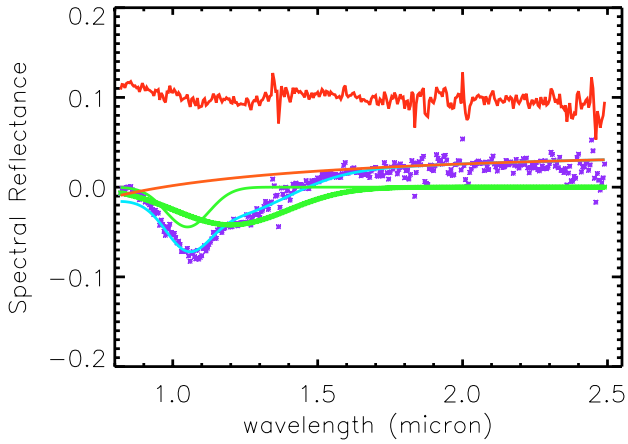

Fig. 3. Modified Gaussian Model applied to asteroid 766 Moguntia. Two absorption bands (light green) associated with olivine were used to model the experimental data, by using free parameters option. The error between the real spectrum and the best fit is presented in red. The best fit (turquoise) suggests a surface dominated by olivine minerals.

E, T or M type asteroid. As a consequence we performed the χ^2 analysis over a wider wavelength range by adding the visible part. Our simulations revealed that a combination of visible and near-infrared data largely attenuates this ambiguity, even for the small density of data in the visible. However, we must be cautious due to the heterogeneity of these visible data (different telescopes, instruments and data reduction procedures).

We complement our NIR spectra with visible spectroscopy, colors and spectrophotometric data as follows: *24 color survey* data were used for 325 Heidelberga and 909 Ulla, *ECAS* colors were used for 1564 Srbija and 766 Moguntia, *SMASS II* data were used for 687 Tinette and 860 Ursina, *S*3*OS*2 for 558 Carmen and 1280 Baillauda, and the visible spectrum presented in Fig. 2 for the asteroid 497 Iva.

The best fit of asteroids and meteorite analogs are presented in Fig. 6, and Table 3 presents the first five best scores for the meteorite analogs with respect to each asteroid, the NIR slope of each asteroid, the V counterpart used in the analysis, and the IRAS albedo when available.

Our results mostly favour metallic meteorites as the best analogs of our asteroid sample (except for 766 Moguntia). As one can see from Table 3, other samples belonging to different meteoritic classes have also been ranked: Murchinson, Tagish Lake, LEW85311 and MAC88177. However, some of these samples have been prepared under particular conditions (heated samples at 700°−800° C for Murchinson, two samples of fresh cut or weathered portion for Tagish Lake meteorite) and we are cautious about their relevance.

Table 3. Best fit of asteroids and meteorite spectra. The five first ranked meteorite analogs have been tabulated. When the meteorite is presented several times in the table for the same asteroid, this represents the differences in preparation of the analyzed sample. Metallic meteorites are the best fit for eight of our asteroids (the exception is the asteroid 766 Moguntia). The table also ranks a heated sample of meteorite Murchinson (marked by *), two samples of fresh cut Tagish Lake meteorite (one of them is presented for several asteroids), one Abee sample, one CM2 meteorite from Antarctica (LEW85311) and one lodranite (MAC88177). The last column show the slope of each asteroid NIR spectrum. We add the IRAS albedo (labeled A) when available.

Spectrum	Meteorite	Type	χ^2 ($\times 10^6$)	S (μm^{-1})
325 Heidelberga	DRP78007	Iron	244	
	Butler	Iron	270	
A = 0.1068	DRP78007	Iron	287	0.27
	DRP78007	Iron	378	
	DRP78007	Iron	415	
497 Iva	Odessa	Iron IA	264	
	Cassey	Iron IAB	613	
	Tagish Lake	CI/CM	698	0.32
	Butler	Iron	993	
	DRP78007	Iron	1280	
558 Carmen	Chulafinnee	Iron IIIAB	86	
	DRP78007	Iron	152	
A = 0.1161	DRP78007	Iron	159	0.256
	DRP78007	Iron	273	
	Feni	Iron	322	
687 Tinette	Chulafinnee	Iron IIIAB	319	
	Feni	Iron	335	
	Feni	Iron	341	0.25
	Tagish Lake	CI/CM	372	
	Tagish Lake	CI/CM	394	
766 Moguntia	Ozona	H6	92	
	ALH84028	CV3	115	
	Murchison*	CM2	147	0.065
	Allende	CV3	189	
	Murchison	CM2	333	
860 Ursina	Murchinson*	CM2	418	
	Abee	E4	471	
	Feni	Iron	507	0.21
A = 0.1618	Feni	Iron	519	
	Odessa	Iron	629	
909 Ulla	Mundrabilla	Iron	218	
	MAC88177	Lodranite	218	
A = 0.0343	Mundrabilla	Iron	262	0.15
	Mundrabilla	Iron	325	
	Murchinson*	CM2	343	
1280 Baillauda	DRP78007	Iron	271	
	Tagish Lake	CI/CM	407	
A = 0.0505	DRP78007	Iron	408	0.27
	DRP78007	Iron	507	
	DRP78007	Iron	508	
1564 Srbija	Odessa	Iron IA	176	
	Odessa	Iron IA	182	
	LEW85311	CM2	408	0.24
	Tagish Lake	CI/CM	416	
	Feni	Iron	421	

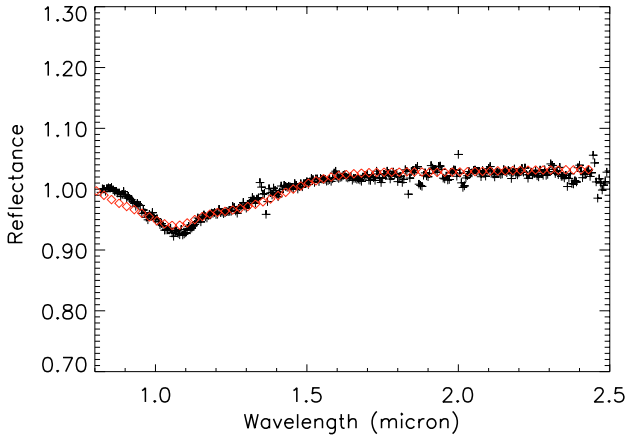

Fig. 4. NIR spectrum of 766 Moguntia (in black) is plotted together with the best fit (red diamonds) obtained using the Shkuratov model (derived composition: 100% olivine with Mg number = 45 ± 5).

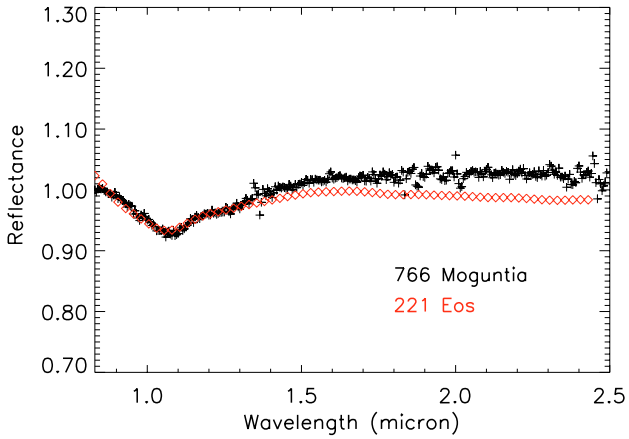

Fig. 5. NIR spectrum of 766 Moguntia presents a trend very similar to the asteroid 221 Eos, classified as a K class member.

The χ^2 results do not settle all the uncertainties concerning the match between M-type asteroids and meteoritic classes. Two meteorite samples (Abee and MAC88177 meteorites) are in good agreement with two spectra (the asteroid 860 Ursina and 909 Ulla respectively). The Abee meteorite has an enstatitic chondritic mineralogy, while MAC88177 has been associated with lodranites. Together with acapulcoites, lodranites are believed to have originated from a parent body that experienced variable degrees of heating, thus being the materialization of a partial melting and melt migration processes (Floss 2000). The brecciated enstatitic chondrite Abee has been classified as EH4, a class that has preserved the original structure of chondrules.

The link between M-asteroids and metallic meteorites does not represent an unique solution, while meteorites experiencing partial melting and several degrees of heating could also give a relatively good fit. In particular, 909 Ulla and 1280 Baillauda have their IRAS albedo in the 0.03−0.05 range, which is compatible with D and T type asteroids but not M-types. For both asteroid spectra the best fit was obtained with an iron meteorite. This result could be biased by the small number of primitive meteorites, assuming that the IRAS albedo is correct.

Particular attention has been paid to the asteroid 766 Moguntia. Its NIR spectrum presents a neutral slope, and a shallow and wider absorption band around 1 μm. This band was previously announced by Hardersen et al. (2006) and their band depth estimation is in agreement with ours

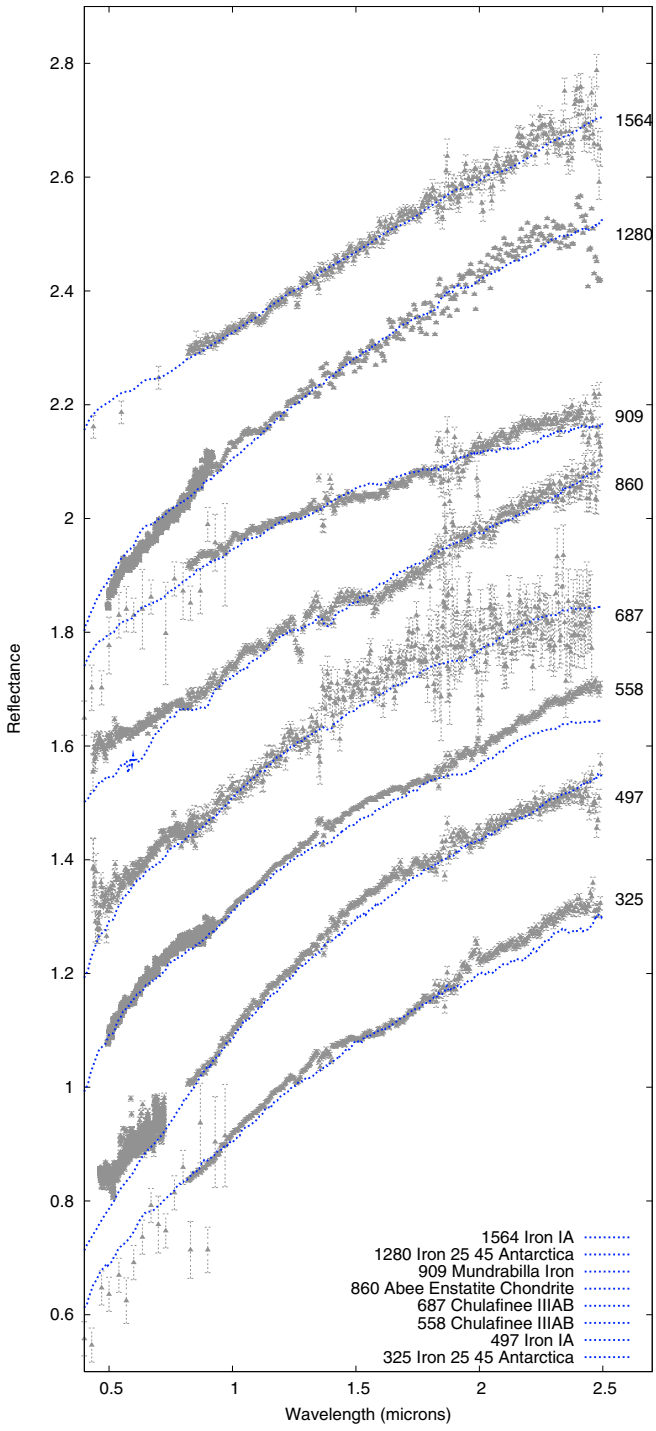

Fig. 6. Spectra of the asteroids presented here and the inferred meteorites (in blue). The legend describing the meteorites corresponds to the best fit, in order, from the top to the bottom. The asteroid visible spectra complement our NIR spectra as discussed in the text.

(around 5%). We underline also the lack of the absorption features in the 2 μm region.

The absorption band at 1 μm suggests the presence of olivine on the asteroid surface. Based on the relative high S/N for 766 Moguntia, a mineralogical analysis has been made using MGM procedures (Sunshine & Pieters 1993).

Nimura et al. (2006) performed an analysis of the Alta'ameem chondritic meteorite in order to constrain the

Table 4. MGM results using two olivine bands. The center of the bands as well as their full width at half maximum (*FWHM*) and strenght are presented. The Fe (%) represents the content of iron in olivine crystals, as derived from the Fig. 1 of Nimura et al. (2006).

Asteroid	Band *I* (*n*m)	*FWHM* (*n*m)	Str	Fe (%)	Band II (*n*m)	*FWHM* (*n*m)	Str	Fe (%)
766 Moguntia	1050.9	178.0	–0.0444	33 ± 1	1201.94	464.5	–0.0421	21 ± 1

olivine bands, by taking into account three of the olivine bands, around 1 μm. Our analysis was started using the same three absorption bands (0.84, 1.050, and 1.190 μm), in the MGM free parameters approach. In this approach, the solution shows that for 766 Moguntia the presence of the 0.84 μm absorption band is unnecessary. Finally, the best solution, adopted and presented in Fig. 3, is deduced with two absorption bands (Table 4). The iron content in the olivine minerals was estimated to be 33% and 21% for each band.

Our MGM analysis is also reinforced by the χ^2 test on RELAB meteorites. The best correspondence of the 766 Moguntia spectrum was found to the Ozona (H6) meteorite sample and ALH84028 (CV3 type). It is unlikely that this object belongs to the M-class.

To investigate in more detail Moguntia's surface composition, we modelled its spectrum using the Shkuratov scattering model (Shkuratov et al. 1999). The first step of the modelling consisted of choosing reasonable end member minerals. We use the optical constants of silicates such as olivine, ortho- and clinopyroxene since the spectra of these minerals display absorption bands in the NIR. For these minerals, we considered the optical constants for different chemistries, i.e., different Mg-number (Lucey 1998). We did not use optical constants of featureless materials (e.g. iron) since no evidence of their existence is brought by Moguntia's NIR spectrum.

The free parameters of the model are the relative abundance of the components (whose sum must be equal to 1), the mineral chemistries of the various components (variation of the Mg-number) and the effective (average) optical pathlength (proportional to the grain size). Finally, an IDL routine using the Levenberg-Marquardt algorithm was used to find the minimum root-mean-squared (RMS) residual between the measured spectrum and the computed one.

The best fit is shown in Fig. 4. Our results imply that Moguntia's surface is composed exclusively of olivine (at a 98% confidence level) with an Mg number of 45 ± 5. The effective (average) optical pathlength is equal to 0.9. This number is considerably low. We interpret this as the presence of 1) a neutral phase which reduces the band depth or 2) a matrix as found in carbonaceous chondrites. Indeed, the CV3 meteorite ALH 84028 provides one of the best matches to Moguntia's spectrum. If confirmed in the visible, this Moguntia-CV3 connection may imply that this asteroid belongs to the K class. The spectra of 221 Eos (R. P. Binzel, Private communication) and 766 Moguntia are very similar and the only variation is due to a slope difference that we may attribute to space weathering effects (Fig. 5). The members of an asteroid family are characterized by similar spectra. The membership of 766 Moguntia in the dynamical family of Eos is also sustained by the good agreement of their spectra. K-type asteroids are spectra intermediate between S and C classes, and Burbine et al. (2001) proposed the K-type asteroids as parent bodies of CO/CV meteorites. This reinforces our conclusion that 766 Moguntia has been misclassified.

5. Conclusions

We obtained nine NIR spectra of asteroids belonging to the M class using IRTF/SpeX and one V spectrum with TNG/Dolores.

Comparative analysis of these objects was performed using a χ^2 method. For one of them, an MGM analysis was also performed.

The NIR spectral slope of eight asteroids span the range $0.15-0.32\,\mu m^{-1}$.

Our spectral observations and analysis confirm a NIR trend of the spectra quite similar to metallic meteorites for eight objects. However, the relatively good match between our targets and some primitive and stony-iron meteorites cannot be completely excluded.

The asteroid 766 Moguntia was investigated using a χ^2 analysis, MGM techniques, and the Shkuratov scattering law. This object presents an absorption feature around 1 μm which could be related to the presence of olivine crystals on its surface. Its NIR spectrum is similar to that of CO/CV meteorites. The similarity of the 766 Moguntia spectrum with the one of 221 Eos, with both objects belonging to the same dynamical family, corresponds to the accepted idea of spectral homegenity within the family.

Acknowledgements. The article is based on observations acquired with InfraRed Telescope Facilities as well as the CODAM remote facilities. The visible spectrum presented herein was obtained using the facilties of Telescopio Nationale Galileo. We thank all the telescope operators for their contribution.
This research utilizes spectra acquired with the NASA RELAB facility at Brown University.
The work of Dan Alin Nedelcu was supported by the ESA traineeship program. We thank Joshua Emery for the useful comments and Richard Binzel and Paul Hardersen for discussions.

References

Barucci, M. A., Capria, M. T., Coradini, A., & Fulchignoni, M. 1987, Icarus, 72, 304
Belskaya, I. N., & Lagerkvist, C.-I. 1996, Planet. Space Sci., 44, 783
Belskaya, I. N., Efimov, Y. S., Lupishko, D. F., & Shakhovskoi, N. M. 1985, Soviet Astron. Lett., 11, 116
Belskaya, I. N., Kiselev, N. N., Lupishko, D. F., & Chernova, G. P. 1987, Kinematika i Fizika Nebesnykh Tel, 3, 19
Belskaya, I. N., Kiselev, N. N., Lupishko, D. F., & Chernova, G. P. 1991, Kinematika i Fizika Nebesnykh Tel, 7, 11
Birlan, M. 2000, Earth Moon and Planets, 88, 1
Birlan, M., Fulchignoni, M., & Barucci, M. A. 1996, Icarus, 124, 352
Birlan, M., Barucci, M. A., Vernazza, P., et al. 2004, New Astron., 9, 343
Birlan, M., Vernazza, P., Fulchignoni, M., et al. 2006, A&A, 454, 677
Bowell, E., Chapman, C. R., Gradie, J. C., Morrison, D., & Zellner, B. 1978, Icarus, 35, 313
Britt, D. T., & Consolmagno, G. J. 2000, Icarus, 146, 213
Burbine, T. H., Binzel, R. P., Bus, S. J., & Clark, B. E. 2001, Meteoritics and Planetary Science, 36, 245
Bus, S. J., & Binzel, R. P. 2002, Icarus, 158, 106
Chapman, C. R., & Gaffey, M. J. 1979, in Asteroids, ed. T. Gehrels, 655
Clark, B. E., Bell, J. F., Fanale, F. P., & O'Connor, D. J. 1995, Icarus, 113, 387
Clark, B. E., Bus, S. J., Rivkin, A. S., Shepard, M. K., & Shah, S. 2004, AJ, 128, 3070

Cloutis, E. A., Gaffey, M. J., Smith, D. G. W., & Lambert, R. S. J. 1990a, J. Geophys. Res., 95, 8323
Cloutis, E. A., Gaffey, M. J., Smith, D. G. W., & Lambert, R. S. J. 1990b, J. Geophys. Res., 95, 281
Cushing, M. C., Vacca, W. D., & Rayner, J. T. 2004, Planet. Space Sci., 116, 362
Dollfus, A., Mandeville, J. C., & Duseaux, M. 1979, Icarus, 37, 124
Floss, C. 2000, Meteoritics and Planetary Science, 35, 1073
Fulchignoni, M., Barucci, M. A., & Tedesco, E. F. 1995, Planet. Sp. Sci., 43, 691
Gaffey, M. J., Cloutis, E. A., Kelley, M. S., & Reed, K. L. 2002, Asteroids III, 183
Gil-Hutton, R. 2007, A&A, 464, 1127
Hardersen, P. S., Gaffey, M. J., & Abell, P. A. 2005, Icarus, 175, 141
Hardersen, P. S., Gaffey, M. J., Cloutis, E., Abell, P. A., & Reddy, V. 2006, in Lunar and Planetary Inst. Technical Report, 37th Annual Lunar and Planetary Science Conference, ed. S. Mackwell, & E. Stansbery, 37, 1106
Harris, A. W. 1979, Icarus, 40, 145
Lagerkvist, C.-I., Belskaya, I., Erikson, A., et al. 1998, A&AS, 131, 55
Lazzaro, D., Angeli, C. A., Carvano, J. M., et al. 2004, Icarus, 172, 179
Lucey, P. G. 1998, J. Geophys. Res., 103, 1703
Lupishko, D. F., & Belskaya, I. N. 1989, Icarus, 78, 395
Magri, C., Nolan, M. C., Ostro, S. J., & Giorgini, J. D. 2007, Icarus, 186, 126
Margot, J. L., & Brown, M. E. 2003, Science, 300, 1939
Nedelcu, D. A., Birlan, M., Vernazza, P., et al. 2007, A&A, 470, 1157
Nimura, T., Hiroi, T., Ohtake, M., et al. 2006, in Lunar and Planetary Institute Conference Abstracts, 37th Annual Lunar and Planetary Science Conference, ed. S. Mackwell, & E. Stansbery, 37, 1600
Ostro, S. J., Hudson, R. S., Nolan, M. C., et al. 2000, Science, 288, 836
Ostro, S. J., Hudson, R. S., Benner, L. A. M., et al. 2002, Asteroids III, 151
Rayner, J. T., Toomey, D. W., Onaka, P. M., et al. 2003, PASP, 115, 362
Rivkin, A. S., Howell, E. S., Britt, D. T., et al. 1995, Icarus, 117, 90
Rivkin, A. S., Howell, E. S., Lebofsky, L. A., Clark, B. E., & Britt, D. T. 2000, Icarus, 145, 351
Rivkin, A. S., Binzel, R. P., Sunshine, J., et al. 2004, Icarus, 172, 408
Shkuratov, Y., Starukhina, L., Hoffmann, H., & Arnold, G. 1999, Icarus, 137, 235
Sunshine, J. M., & Pieters, C. M. 1993, J. Geophys. Res., 98, 9075
Tedesco, E. F., & Veeder, G. J. 1992, in The IRAS Minor Planet Survey, Tech. Rep.PL-TR-92-2049, Phillips Laboratory, Hanscom AF Base, MA, ed. E. F. Tedesco, G. J. Veeder, J. W. Fowler, & J. R. Chillemi, 1, 313
Tholen, D. J. 1984, Ph.D. Thesis, AA(Arizona Univ., Tucson.)
Tholen, D. J. 1989, in Asteroids II, ed. R. P. Binzel, T. Gehrels, & M. S. Matthews, 1139
Tholen, D. J., & Barucci, M. A. 1989, in Asteroids II, ed. R. P. Binzel, T. Gehrels, & M. S. Matthews, 298
Vacca, W. D., Cushing, M. C., & Rayner, J. T. 2004, PASP, 116, 352
Zellner, B., Tholen, D. J., & Tedesco, E. F. 1985, Icarus, 61, 355